THE JOURNAL OF BIOLOGICAL CHEMISTRY VOL. 284, NO. 49, pp. 34244–34256, December 4, 2009

Dynamic Interaction of Amphiphysin with N-WASP Regulates Actin Assembly*[S]

Received for publication, September 8, 2009, and in revised form, September 8, 2009 Published, JBC Papers in Press, September 16, 2009, DOI 10.1074/jbc.M109.064204

Hiroshi Yamada,[a] Sergi Padilla-Parra,[b] Sun-Joo Park,[c,d] Toshiki Itoh,[e] Mathilde Chaineau,[b,f1] Ilaria Monaldi,[g,h] Ottavio Cremona,[i2] Fabio Benfenati,[g,h2] Pietro De Camilli,[j] Maïté Coppey-Moisan,[b] Marc Tramier,[b] Thierry Galli,[b,f] and Kohji Takei[a3]

From the [a]Department of Neuroscience, Okayama University Graduate School of Medicine, Dentistry, and Pharmaceutical Sciences, 2-5-1 Shikata-cho, Kita-ku, Okayama 700-8558, Japan, [b]Institut Jacques Monod, UMR 7592, CNRS, Université Paris-Diderot and Université Pierre et Marie Curie, 75205 Paris Cedex 13, France, [c]Division of Lipid Biochemistry, Kobe University Graduate School of Medicine, 7-5-1 Kusunoki-cho, Chuo-ku, Kobe 650-0017, Japan, the [d]Department of Chemistry, Pukyong National University, 599-1 Daeyeon 3-Dong, Busan 608-737, Korea, [e]Division of Membrane Biology, Kobe University Graduate School of Medicine, 7-5-1 Kusunoki-cho, Chuo-ku, Kobe 650-0017, Japan, [f]Membrane Traffic in Neuronal and Epithelial Morphogenesis, INSERM U950, F-75013 Paris, France, the [g]Department of Neuroscience and Brain Technologies, Italian Institute of Technology, Via Morego 30, 16163 Genova, Italy, the [h]Department of Experimental Medicine, University of Genova and Istituto Nazionale di Neuroscienze, Viale Benedetto XV, 3, 16132 Genova, Italy, [i]Fondazione Italiana Ricerca sul Cancro Institute of Molecular Oncology, Universitá Vita-Salute San Raffaele and Istituto Nazionale di Neuroscienze, 20141 Milano, Italy, and the [j]Department of Cell Biology and Neurobiology, Howard Hughes Medical Institute, Yale University School of Medicine, New Haven, Connecticut 06510

Amphiphysin 1, an endocytic adaptor concentrated at synapses that couples clathrin-mediated endocytosis to dynamin-dependent fission, was also shown to have a regulatory role in actin dynamics. Here, we report that amphiphysin 1 interacts with N-WASP and stimulates N-WASP- and Arp2/3-dependent actin polymerization. Both the Src homology 3 and the N-BAR domains are required for this stimulation. Acidic liposome-triggered, N-WASP-dependent actin polymerization is strongly impaired in brain cytosol of amphiphysin 1 knock-out mice. FRET-FLIM analysis of Sertoli cells, where endogenously expressed amphiphysin 1 co-localizes with N-WASP in peripheral ruffles, confirmed the association between the two proteins *in vivo*. This association undergoes regulation and is enhanced by stimulating phosphatidylserine receptors on the cell surface with phosphatidylserine-containing liposomes that trigger ruffle formation. These results indicate that actin regulation is a key function of amphiphysin 1 and that such function cooperates with the endocytic adaptor role and membrane shaping/curvature sensing properties of the protein during the endocytic reaction.

The dynamic nature of the actin cytoskeleton is crucial for a variety of cellular events, including cell morphogenesis, cell migration, and intracellular membrane traffic (1). Actin polymerization is stimulated by a variety of actin regulatory proteins, prominent among which are WASP family proteins that function by triggering Arp2/3-mediated actin nucleation (2). Activation of WASP family proteins, in turn, is controlled by factors that bind these proteins and release an autoinhibitory intramolecular interaction that prevents their VCA domain from interacting with the Arp2/3 complex. As extensively shown for N-WASP, many such factors are proteins that bind to the N-WASP proline-rich region via the SH3[4] domain.

Recently, we have found that the SH3 domain containing protein amphiphysin 1 stimulates actin polymerization during phagocytosis in testicular Sertoli cells, and this effect requires interactions of its C-terminal SH3 domain (3). Amphiphysin 1 is an endocytic adaptor present at high levels in brain at neuronal synapses but is also expressed at significant levels in Sertoli cells (4, 5). In addition to a C-terminal SH3 domain, known to bind the GTPase dynamin and the phosphoinositide phosphatase synaptojanin (6), amphiphysin 1 contains an N-terminal BAR domain, a curved protein module that binds lipid bilayers and generates and senses curvature (7, 8). It also contains binding motifs for clathrin and for the clathrin adaptor AP-2 (9). Hence, amphiphysin 1 was primarily studied as an endocytic protein capable of assembling at the neck of endocytic pits and of coupling clathrin-mediated budding to dynamin-mediated fission (10, 11). However, regulatory roles of amphiphysin 1 in actin cytoskeleton have also been suggested by studies of neuronal growth cones (12) and by the function of the amphiphysin homologue in yeast, Rvs167 (13–15).

* This work was supported, in whole or in part, by a National Institutes of Health grant (to P. D. C.). This work was also supported in part by grants from the Ministry of Education, Science, Sports, and Culture of Japan, a grant from the United States-Japan Brain Research Collaborative (to K. T.), grants from INSERM (to T. G.), an INSERM-Japan Society for the Promotion of Science grant (to K. T. and T. G.), grants from Foundation pour la Recherche Médicale and from CNRS (to M. C. M.), European Union-Marie-Curie Fellowship MRTN-CT-2005-019481 (to S. P. P.), grants from Ministero dell'Istruzione, dell'Università e della Ricerca (Italy) (to F. B. and O. C.), grants from Compagnia di San Paolo, Torino, Italy (to F. B.), and by Basic Science Research Program through the National Research Foundation of Korea funded by the Ministry of Education, Science, and Technology Grant 2009-0065739 (to S. P.).

[S] The on-line version of this article (available at http://www.jbc.org) contains supplemental Figs. S1 and S2 and Movie S1.

[1] Supported by the Association pour la Recherche sur le Cancer.
[2] Supported by Telethon (Italy).

[3] To whom correspondence should be addressed. Tel.: 81-86-235-7120; Fax: 81-86-235-7126; E-mail: kohji@md.okayama-u.ac.jp.

[4] The abbreviations used are: SH3, Src homology 3; GFP, green fluorescent protein; GST, glutathione *S*-transferase; PS, phosphatidylserine; PI, phosphatidylinositol; PI(4,5)P_2, phosphatidylinositol 4,5-bisphosphate; PC, phosphatidylcholine; PBS, phosphate-buffered saline; FRET-FLIM, fluorescence resonance energy transfer-fluorescence lifetime imaging microscopy; Ni-NTA, nickel-nitrilotriacetic acid; WT, wild type.

We have searched for a mechanistic explanation of the stimulatory action of amphiphysin 1 on actin dynamics. We now show that amphiphysin 1 acts as an activator of N-WASP, and we provide evidence for the occurrence of this activation in living cells.

EXPERIMENTAL PROCEDURES

Reagents and Antibodies—Phosphatidylinositol (4,5)-bisphosphate (PI(4,5)P_2) from bovine brain was purchased from Calbiochem (Darmstadt, Germany). PS, phosphatidylethanolamine, phosphatidic acid, phosphatidylinositol (PI), and phosphatidylcholine (PC) were from Avanti Polar Lipids (Alabaster, AL). Glutathione-Sepharose 4B beads, pGEX-6P vector, PreScission protease, and thrombin were from GE Healthcare. Rabbit anti-Myc antibodies were purchased from Santa Cruz Biotechnology (Santa Cruz, CA). Monoclonal anti-amphiphysin 1 antibodies (monoclonal antibody 3) were as described previously (3). Rabbit anti-PAN-WAVE antibody was a kind gift from Dr. Scita (IFOM Istituto Fondazione Italiana Ricerca sul Cancro di Oncologia Molecolare Via Adamello 16, Italy). Rabbit anti-N-WASP antibody was a kind gift from Dr. Kirschner (Harvard Medical School, Boston, MA). Anti-synaptophysin and anti-dynamin 1 antibodies were purchased from Sigma and Synaptic Systems (Goettingen, Germany), respectively. Wiskostatin was purchased from EMD Biosciences, Inc. (Darmstadt, Germany).

Animals and Cell Culture—Wild type mice were purchased from Shimizu Laboratory Supplies Co. (Kyoto, Japan). Amphiphysin 1 knock-out mice (amphiphysin $1^{-/-}$) were generated by gene targeting in embryonic stem cells as described previously (16). Ten-week-old wild type or amphiphysin $1^{-/-}$ brains were used for cytosol preparation. All animals were maintained in clean conditions with free access to food and water. They were allowed to adapt to their environment for more than 1 week before initiating the experiments. Ser-W3 cells, a rat Sertoli cell line, were cultured with Dulbecco's modified Eagle's medium containing 10% fetal bovine serum at 37 °C under 5% CO_2 (3).

Protein Purification—N-WASP was expressed in Sf9 cells by a Bac-to-Bac baculovirus expression system (Invitrogen) with a His_6 tag. Recombinant virus-infected Sf9 cells were lysed, and His_6-N-WASP was purified with Ni-NTA-agarose (Qiagen). GST fusion VCA was purified as described previously (17, 18). Arp2/3 complex was purified as described previously (19). Actin was purified from rabbit skeletal muscle, and monomeric actin (G-actin) was isolated by gel filtration on Superdex 200 (GE Healthcare) in G buffer (2 mM Tris-HCl, pH 8.0, 0.2 mM $CaCl_2$, 0.5 mM dithiothreitol, 0.2 mM ATP). Full-length amphiphysin 1, 1–306 amino acids (N-BAR-PRS), 1–626 amino acids (ΔSH3), 226–695 amino acids (ΔN-BAR), and Δ248–601 amino acids (N-BAR-SH3) were subcloned into the plasmid pGEX-6P as described previously (8). The SH3 domain was subcloned into the pGEX-2T vector. The nucleotide sequences of the constructs were verified using a DNA sequence analyzer. The expression of GST fusion proteins was induced by 0.1 mM isopropyl 1-thio-D-galactopyranoside at 37 °C for 3–6 h in LB medium supplemented with 100 μg/ml ampicillin at $A_{600} = 0.8$. The purification of GST fusion proteins was performed as described previously (9), and the cleavage of the GST with PreScission protease was carried out according to the manufacturer's instruction. Finally, the proteins were purified on Mono Q column equilibrated in 20 mM Tris-HCl, pH 7.7, and 0.2 M NaCl. The protein solution (1 mg/ml protein) was stored at −80 °C and thawed at 37 °C before use. The purity of these proteins was confirmed by SDS-PAGE.

cDNA Constructs and Transfection—Full-length amphiphysin 1 or 1–626 amino acids (ΔSH3) containing the BamHI and EcoRI restriction sites were subcloned into a pEGFP-C1 vector (Clontech) or mCherry-C1 kindly gifted by Dr. Tsien (Howard Hughes Medical Institute, University of California, San Diego). In another case, amphiphysin 1 containing XhoI and EcoRI restriction sites was subcloned into mCherry-N1. The plasmids pEF-BOS-myc-N-WASP and pEGFP-N-WASP were described previously (20). Full-length N-WASP and 265–391 amino acids (PRD of N-WASP) containing XhoI and EcoRI restriction sites were subcloned into mCherry-C1. The nucleotide sequences of the constructs were verified using DNA sequence analysis. The constructs were transfected into Ser-W3 cells using a Lipofectamine 2000 transfection system (Invitrogen). For FRET-FLIM analysis, Ser-W3 cells (7×10^4 cells per well) were co-transfected with 3 μg of plasmids containing cDNA for GFP-tagged protein and 1 μg of cDNA for mCherry-tagged protein. Four μg of GFP-amphiphysin 1 were transfected as a negative control. Twenty four hours after transfection, cells were subjected to FRET analysis.

Preparation of Liposomes—For stimulation of Ser-W3 cells, small unilamellar liposomes containing 70% PC and 30% PS were prepared by sonication as described previously (3). For actin polymerization assay, small liposomes of uniform size, ~100 nm in diameter, composed of 50% PS/50% PC, 50% phosphatidylethanolamine/50% PC, 50% PI/50% PC, 50% phosphatidic acid/50% PC, or 10% PI(4,5)P_2/90% PC were used. For this purpose, large unilamellar liposomes in 1 mM EDTA, 20 mM Hepes, pH 7.4, were prepared as described previously (21) and then extruded in a syringe-type extruder (Avanti Polar Lipids) six times through polycarbonate membranes (pore size, 100 nm).

Quantification of Membrane Ruffle Formation—Ser-W3 cells (1×10^4 cells/coverslip) in serum-free Dulbecco's modified Eagle's medium were stimulated with 0.25 mM PS-containing liposomes and incubated at 37 °C for 10 min. The cells were then washed with PBS containing 1.5 mM $CaCl_2$ and 1 mM $MgCl_2$ (PBS(+)) three times, fixed with 4% paraformaldehyde, permeabilized, and stained with Alexa 488-phalloidin or anti-c-Myc antibodies. Formed ruffles were characterized as thick actin filament accumulation at the cell periphery (3). To quantify ruffle formation, cells that had no ruffles were scored as negative, whereas cells that had one or more ruffles were considered to be positive. The number of ruffle-positive cells were counted and expressed as a percentage of total number of cells analyzed. At least 100 cells in different areas of the wells were counted in each experiment.

Microscopy—Ser-W3 cells (1×10^4 cells/coverslip) were fixed with 4% paraformaldehyde in PBS(+) at room temperature, permeabilized with 0.1% Triton X-100, and double stained by immunofluorescence as described previously (22). The samples were examined using a spinning disk confocal microscope system

(CSU10, Yokogawa Electric Co., Japan) combined with an inverted microscope (IX-71, Olympus Optical Co., Ltd., Japan) and a CoolSNAP-Pro camera (Roper Industries, Sarasota, FL). The system was steered by Metamorph software (Molecular Devices). When necessary, images were further processed using Adobe Photoshop and Illustrator software.

Preparation of Brain Cytosol—Brain cytosol was prepared as described previously (23). Briefly, 20 brains of wild type or amphiphysin 1 knock-out mice were homogenized in 5 ml of XB buffer (10 mM Hepes, 100 mM KCl, 2 mM $MgCl_2$, 0.1 mM $CaCl_2$, 5 mM EGTA, 50 mM sucrose, 1 mM dithiothreitol, 1 μg/ml leupeptin, 5 μg/ml pepstatin, and 0.4 mg/ml phenylmethylsulfonyl fluoride), pH 7.4. The homogenate was centrifuged at 3,000 $\times$ *g* for 20 min and 10,000 $\times$ *g* for 20 min. The resultant supernatant was diluted with XB buffer up to 4-fold and centrifuged at 400,000 $\times$ *g* for 1 h. The clear supernatant was carefully collected and re-concentrated to one-fourth the volume using Centriprep-10 concentrators (Amicon Corp.). A final concentration of the cytosol was 40–50 mg/ml. Amounts of actin in wild type or amphiphysin $1^{-/-}$ brain cytosol were estimated to be equal by Western blotting.

Preparation of Synaptosomes—Synaptosomes from adult mouse cortices were purified from P2 fractions by centrifugation on discontinuous Percoll gradients as described previously (24) with 0.5 mM EGTA in the initial homogenization buffer. The final synaptosomal pellet was resuspended in resting buffer (20 mM Hepes, 145 mM NaCl, 5 mM KCl, 1 mM $MgCl_2$, 0.1 mM EGTA, 10 mM glucose, pH 7.4) to yield a synaptosome suspension with an OD_{750} = 0.75–0.85.

Determination of Actin Levels in Synaptosomes—G-actin/F-actin cycling was evaluated using a procedure described previously (25) with some modifications. One-ml

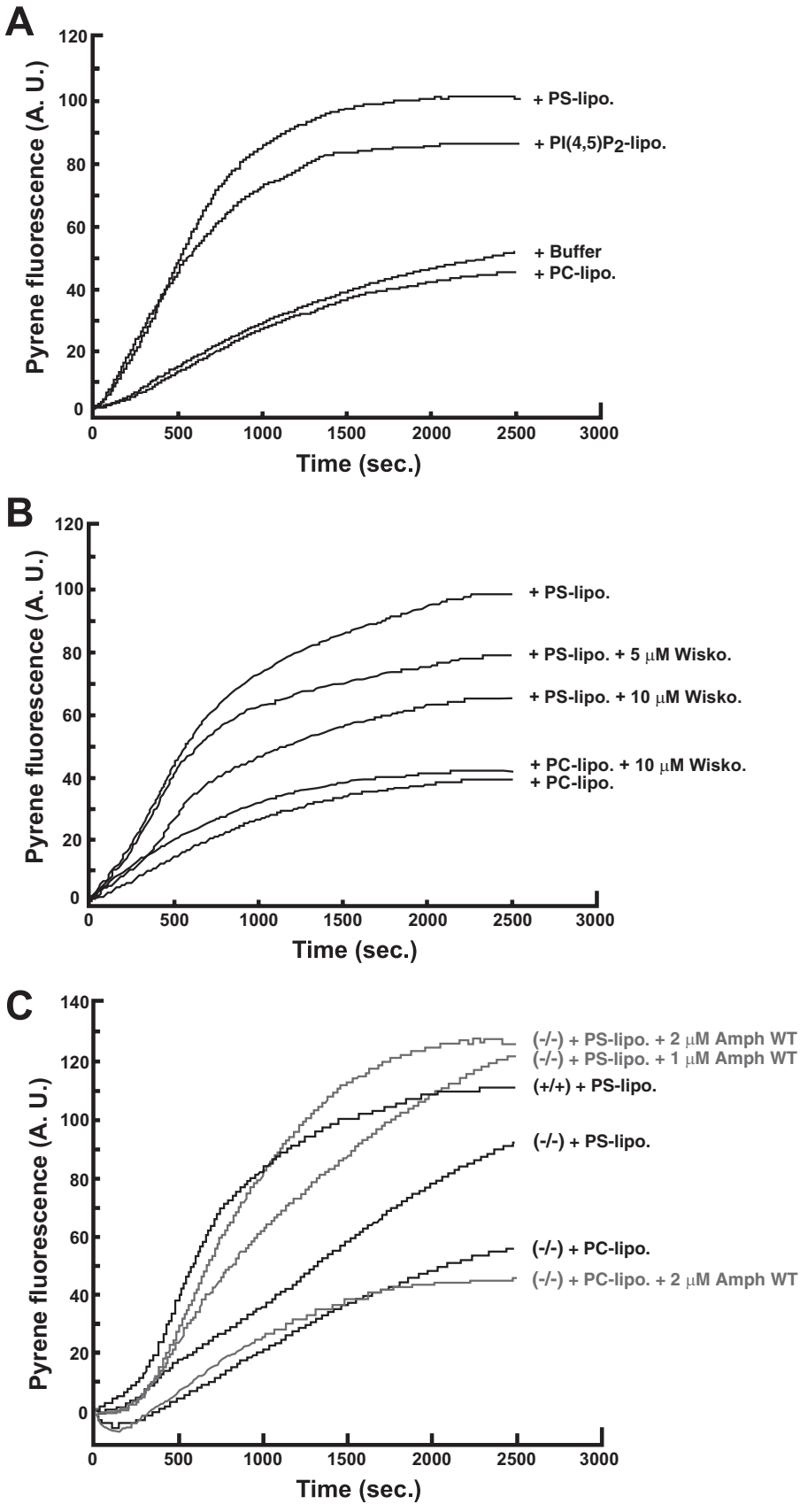

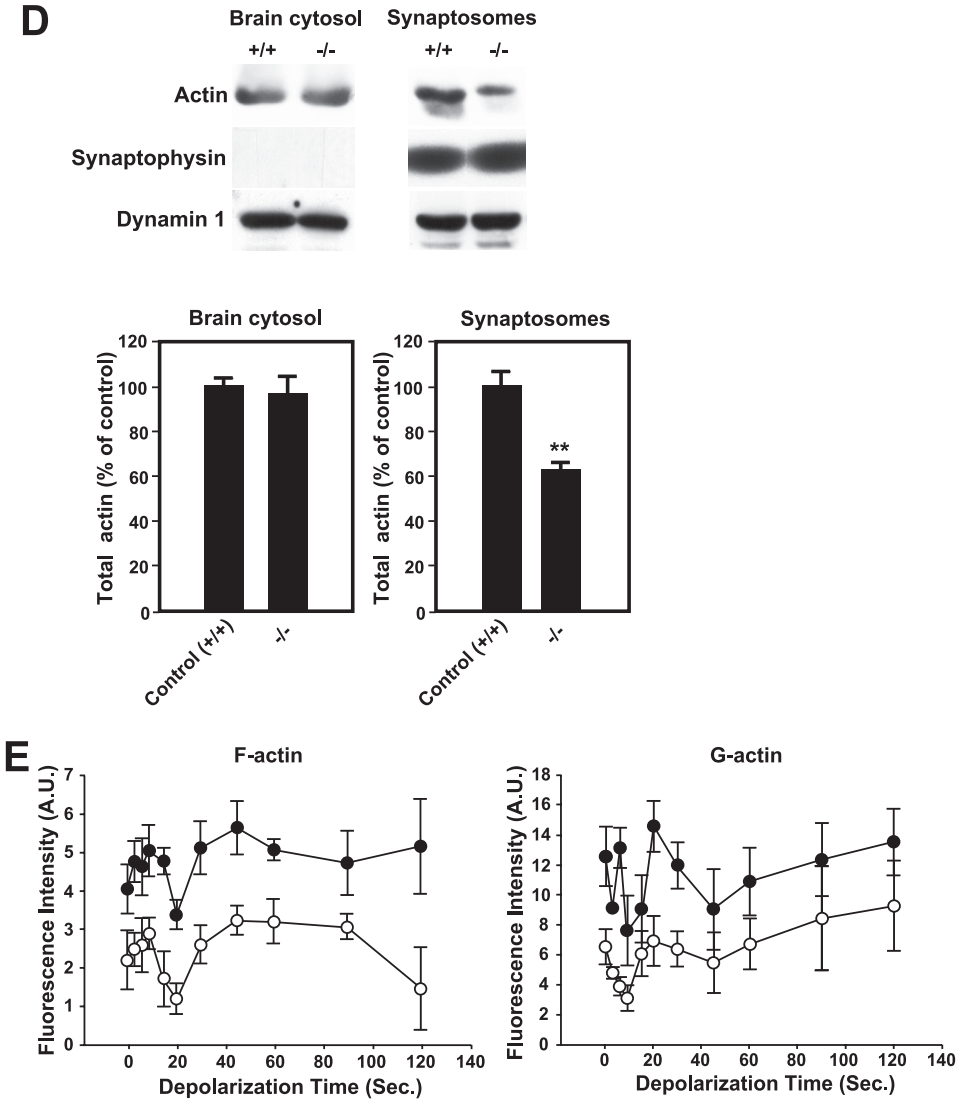

FIGURE 1—*continued*

aliquots of the synaptosome stock were preincubated at 30 °C for 20 min and collected by centrifugation at 10,000 × *g* for 20 s. Synaptosomes were resuspended in 70 μl of depolarizing buffer (20 mM Hepes, 75 mM NaCl, 75 mM KCl, 2 mM $CaCl_2$, 1 mM $MgCl_2$, 10 mM glucose, pH 7.4) and fixed by the addition of 120 μl of 2.5% glutaraldehyde at various times of depolarization (from 3 to 120 s). For the zero time point, depolarizing buffer and glutaraldehyde were combined before the resuspension of the synaptosomal pellet. Synaptosomes were sedimented and subsequently permeabilized in 0.1% Triton X-100 (v/v) and 1 mg/ml $NaBH_4$ in resting buffer for 2–3 min. The buffer was removed, and rhodamine-phalloidin or Oregon Green-DNase I (Invitrogen) in 5 mM KCl, 145 mM NaCl, 2 mM $CaCl_2$ was added (final volume 100 μl). Staining for 20 min in the dark at room temperature was followed by 1–2 washes with 500 μl of resting buffer. Labeled synaptosomes were resuspended in 0.32 M sucrose and stored in the dark at 4 °C. The fluorescence associated with the samples was measured 24 h later using an LS50 spectrofluorometer (PerkinElmer Life Sciences) at the excitation and emission wavelengths of 540 and 566 nm for rhodamine-phalloidin and 497 and 524 nm for Oregon Green-DNase I, respectively (with 2.5 and 5 nm excitation/emission slits).

In Vitro Actin Assembly Assay—For quantitative analysis of actin assembly using cytosol, pyrene-actin assay was carried out according to Ma *et al.* (26). Briefly, diluted cytosol (8 mg/ml) with XB buffer supplemented with 0.4 mg/ml pyrene-actin (Cytoskeleton Inc.), 1.3 mM $MgCl_2$, 0.1 mM EGTA, and ATP-generating system (1 mM ATP, 8 mM creatine phosphate, 8 units/ml phosphocreatine kinase) was incubated in a quartz cuvette at room temperature for 10 min. Lipid membrane at the indicated concentration was added, and pyrene fluorescence was then measured at 407 nm with excitation at 365 nm in an F-2500 fluorescence spectrophotometer (Hitachi Co. Ltd., Japan) with a 10-nm slit width. Pyrene-actin assays for N-WASP-dependent Arp2/3 activation were performed as described previously (20).

FIGURE 1. **Actin dynamics is reduced in amphiphysin $1^{-/-}$ in synapse and brain cytosol.** *A,* liposome-induced actin polymerization measured by pyrene fluorescence. Wild type brain cytosols were treated with 100 μM liposomes composed of 50% PS and 50% PC (+*PS-lipo.*) or 90% PC and 10% PI(4,5)P_2 (+*PI(4,5)P_2-lipo.*). As controls, the incubation was carried out in the presence of 100 μM 100% PC (+*PC-lipo.*) or in the absence of liposomes (+*Buffer*). Time 0 indicates the time when the liposomes were added. *B,* inhibition of PS-induced actin polymerization by wiskostatin. Brain cytosol was pretreated with 5 or 10 μM wiskostatin (*Wisko.*) for 10 min. Then, the cytosol was stimulated with PS-liposomes or PC-liposomes. *C,* reduction of actin polymerization in amphiphysin $1^{-/-}$ brain cytosol ((−/−) + *PS-lipo.*). The reduction was recovered in the presence of PS by adding back 1 or 2 μM of recombinant full-length amphiphysin to the amphiphysin $1^{-/-}$ cytosol. The incubation was carried out as in *B. D,* actin, but not dynamin 1 and synaptophysin, was decreased in amphiphysin $1^{-/-}$ synaptosomes. Quantitative comparison of actin levels in total brain cytosol (*left panel*, $n = 8$ for both genotypes) and synaptosomes (*right panel*, $n = 4$ for both genotypes) from WT or amphiphysin $1^{-/-}$ mice. Twenty μg of each fraction per lane were analyzed. Representative Western blots using antibody directed against actin, synaptophysin, or dynamin 1 were shown (*upper panel*). The amount of actin was measured by densitometry. Statistical significance was determined by Student's *t* tests (**, $p < 0.01$). *E,* cycling of actin assembly in depolarized synaptosomes. Synaptosomes from of WT (*closed circles*) and amphiphysin $1^{-/-}$ mice (*open circles*) were depolarized with high K^+ for the indicated times. Amounts of F-actin (*left panel*) and G-actin (*right panel*) were fluorometrically measured by rhodamine-phalloidin and Oregon Green-DNase I, respectively. Each data point represents the mean ± S.E. of the fluorometric readings performed from 10 independent experiments.

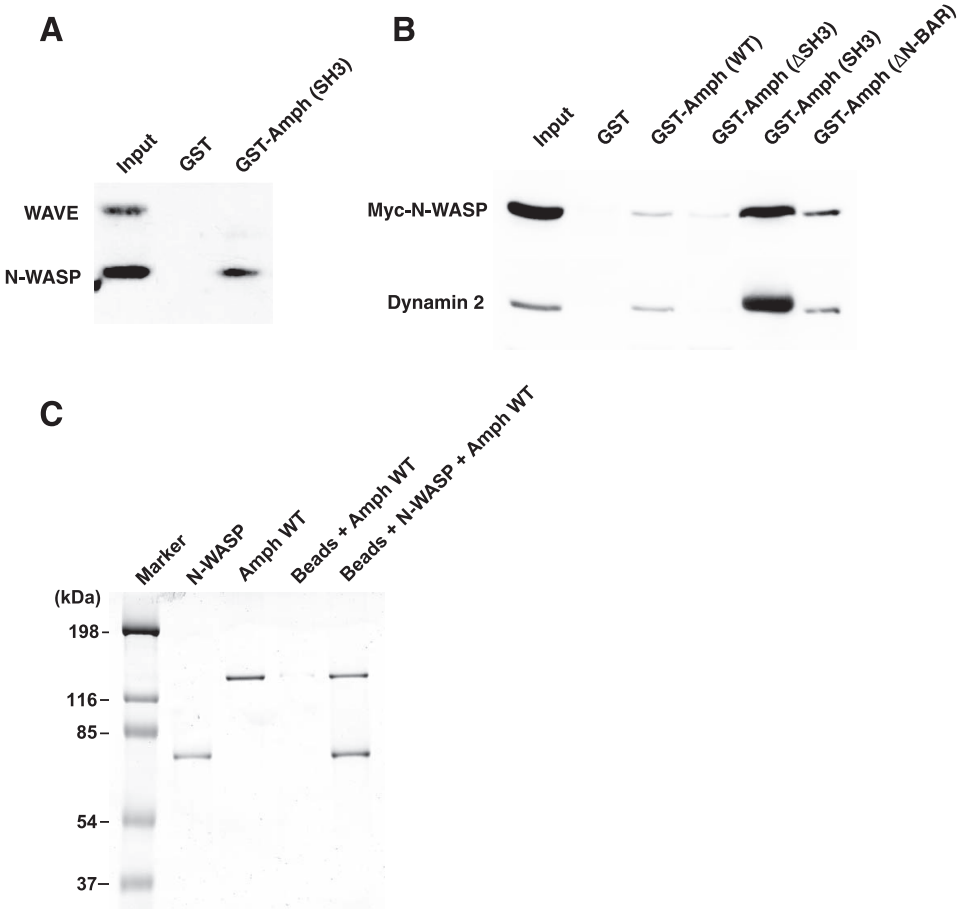

FIGURE 2. **Amphiphysin 1 directly interacts with N-WASP.** SH3-mediated binding of amphiphysin 1 (*Amph*) with N-WASP in synaptosomes (*A*) and Sertoli cells (*B*). *A,* Western blot analysis of a representative pulldown experiment from RIPA extracts of rat brain synaptosomes (2 mg of protein/sample) with GST or GST fused to the SH3 domains of amphiphysin 1 (5 nmol of fusion protein/sample preadsorbed to 60 μl of GSH-Sepharose). Wave was used as a negative control. Proteins that bound to GSH beads were probed with antibodies recognizing both endogenous N-WASP and WAVE. The *1st lane* (*Input*) shows the total amount of N-WASP and WAVE in the starting material. The experiments were performed five times with similar results. *B,* 300 μg of GST-Amph (*WT*), GST-Amph (Δ*SH3*), GST-Amph (*SH3*), GST-Amph (Δ*N-BAR*), or GST bound to GSH beads were incubated with 0.7 mg of Ser-W3 cell lysates transfected with myc-N-WASP proteins solubilized by 1% Triton X-100 for 2 h. N-WASP bound to the beads was analyzed by Western blotting with antibodies against Myc. The same samples were analyzed using anti-dynamin 2 antibodies. *C,* pulldown experiments using purified proteins. His_6-N-WASP at 100 μg was incubated with 50 μl of Ni-NTA beads for 1 h at 4 °C. After gentle washing, 20 μl of His_6-N-WASP-bound Ni-NTA beads or Ni-NTA beads alone were incubated with 50 μg of amphiphysin WT in PBS (pH 8.0) containing 0.01% Tween 20 at 4 °C for 2 h. N-WASP and amphiphysin WT (*Amph WT*) bound to the beads were separated by SDS-PAGE and stained with Coomassie Brilliant Blue. Five hundred ng of His_6-N-WASP or amphiphysin WT were loaded as standards.

Multifocal Multiphoton Fluorescence Lifetime Imaging Microscopy and Data Analysis—The FRET-FLIM system was described previously (27). Briefly, the FRET-FLIM apparatus combines multifocal multiphoton excitation (TriMscope, LaVision Biotec, Bielefeld, Germany) and a fast-gated CCD camera (Picostar, LaVision Biotec, Bielefeld, Germany). Two-photon multifocal excitation was carried out using the TriMScope connected to an inverted microscope (IX 71, Olympus, Tokyo, Japan). A mode-locked Ti:Sa laser at 950 nm for the excitation of GFP (Spectra Physics, France) was split into 2–64 beams by utilizing a 50/50 beam splitter and mirrors. A line of focus was then created at the focal plane, which can be scanned across the sample. A filter wheel of spectral filters (535AF45 for GFP) was used to select the fluorescence imaged onto a fast-gated light intensifier connected to a CCD camera. All instrumentation was controlled by IMSpector software developed by LaVision Biotec. Analysis of the data was done by using Image-J. Quantitative analysis was carried out as described previously (27). Briefly, the images from a time-gated stack are first smoothed by a 3 × 3 mask to decrease the noise. After that, Equation 1 was applied on the resulting background-subtracted time-gated images to recover mean lifetime pixel by pixel.

$$\langle\tau\rangle = \sum \Delta t_i \cdot I_i / \sum I_i \quad \text{(Eq. 1)}$$

Finally, Equation 2 was applied on mean lifetime images using fixed lifetime donor values (τ_D) to recover mf_D. The quantity mf_D stands for the minimal percentage of donor engaged in FRET.

$$mf_D = (1 - (\langle\tau\rangle/\tau_D))/((\langle\tau\rangle/2\cdot\tau_D) - 1)^2 \quad \text{(Eq. 2)}$$

The mf_D was an interesting parameter because it retrieves information about a known threshold of interacting donor protein. In this study, mf_D stands for the minimal percentage of amphiphysin 1/amphiphysin 1 interaction and the minimal percentage of amphiphysin 1/N-WASP interaction.

RESULTS

Amphiphysin 1 Is Implicated in N-WASP-dependent Actin Assembly—Incubation of liposomes containing acidic phospholipids with cytosol in the presence of ATP results in a powerful polymerization of actin that can be monitored by pyrene fluorescence assay (supplemental Fig. S1) (3, 28). Time courses of the PS- or PI(4,5)P_2-induced actin polymerization are shown in Fig. 1*A*. The actin polymerization in the presence of PS, but not PC, was inhibited by wiskostatin, an N-WASP inhibitor (Fig. 1*B*) (29). To determine the impact of amphiphysin 1 on this lipid bilayer-induced actin polymerization, we compared the effect of brain cytosol obtained from WT or amphiphysin 1 knock-out mice (amphiphysin $1^{-/-}$). Amphiphysin $1^{-/-}$ cytosol is almost completely devoid of not only amphiphysin 1 but also amphiphysin 2, a major brain-specific isoform that forms a heterodimer with amphiphysin 1 (16). PS-dependent actin polymerization in amphiphysin $1^{-/-}$ cytosol was reduced by ~60% compared with wild type cytosol at the 1500-s time point (Fig. 1*C*). The decrease was rescued by supplementing the amphiphysin $1^{-/-}$ cytosol with recombinant amphiphysin 1 (Fig. 1*C*). In the pres-

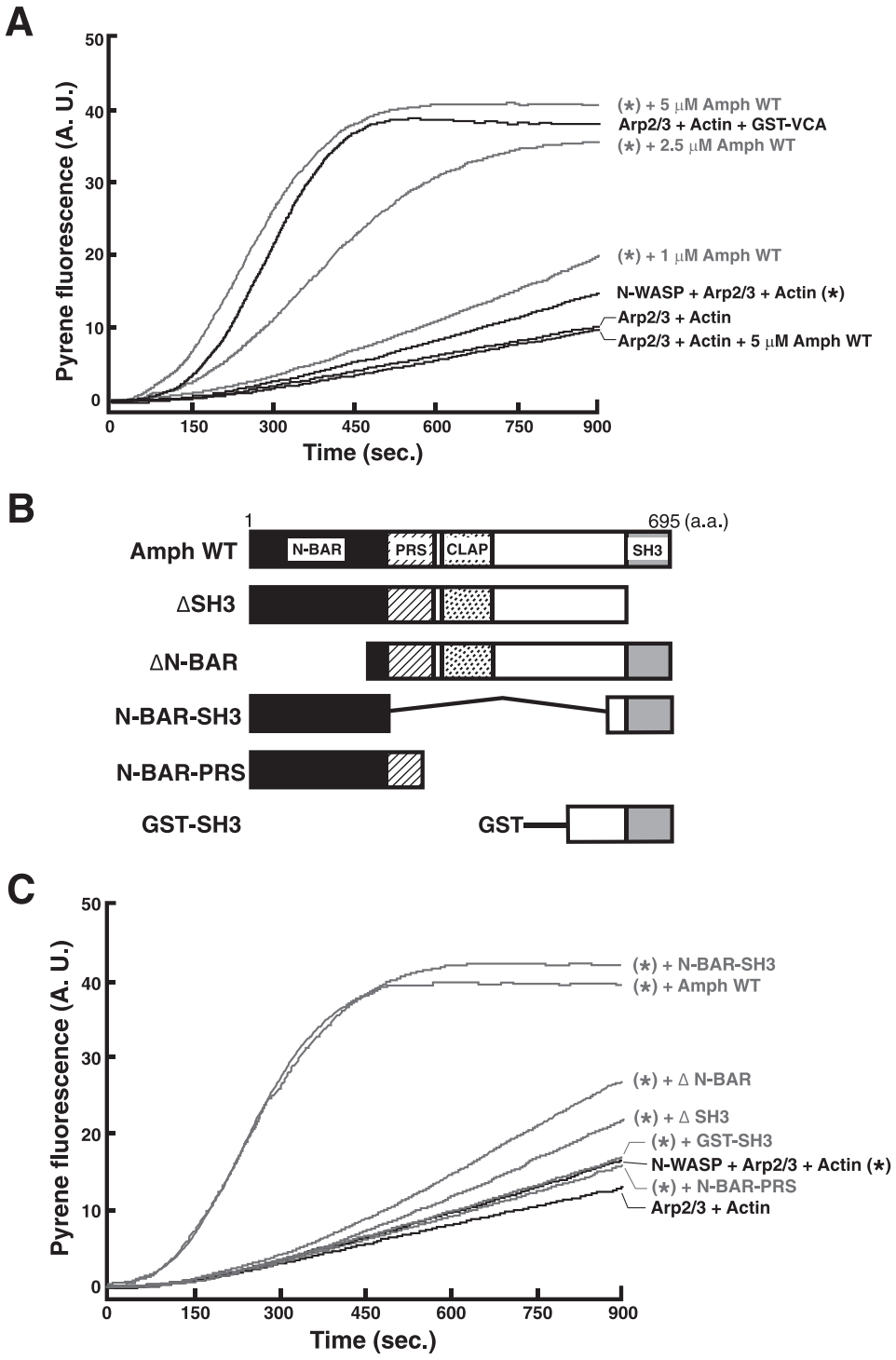

FIGURE 3. **Amphiphysin 1 stimulates N-WASP-dependent actin assembly.** *A,* actin polymerization with 60 nM Arp2/3 complex and 100 nM N-WASP in XB buffer was examined in the presence of various concentrations of recombinant amphiphysin 1 (+*Amph WT*). One hundred nM GST-VCA was used as positive control as described previously (20, 44). *B,* domain structures of the amphiphysin 1 constructs used in *C*. *N-BAR*, N-terminal amphipathic helix preceding the consensus BAR (BIN/amphiphysin/Rvs) domain; *PRS*, proline-rich stretch; *CLAP*, clathrin-AP2-binding domain; *SH3,* Src homology 3. *C,* both N-BAR and SH3 domain are required for stimulating N-WASP-dependent actin assembly. Actin polymerization with Arp2/3 complex and N-WASP proteins was examined as described in *A* using 5 μM of mutant proteins.

ence of PC-liposomes, the supplementation of amphiphysin 1 showed no effect (Fig. 1*C*). Furthermore, addition of the same amount of amphiphysin 1 to WT cytosol did not alter PS-dependent actin polymerization (supplemental Fig. S2). Thus, amphiphysin is implicated in PS-dependent actin polymerization, and N-WASP is likely to be involved in this process.

Because both amphiphysin 1 and N-WASP are concentrated at the synapse (30, 31), we investigated whether the lack of amphiphysin affects the formation of F-actin in synaptosomes. The amount of actin in total brain cytosol was essentially the same in WT or amphiphysin $1^{-/-}$ mice (Fig. 1*D, upper left panel*). In synaptosomes, however, actin was selectively reduced in amphiphysin $1^{-/-}$ (Fig. 1*D, upper right panel*). Despite the reduced level of actin, the activity-dependent cycling of actin assembly was not changed in amphiphysin $1^{-/-}$ synaptosomes (Fig. 1*E*). Indeed, in both WT and amphiphysin $1^{-/-}$ synaptosomes, F-actin levels showed an early peak (10 s after depolarization), a drop, and a later peak (30–40 s after depolarization), although the fluorescence levels were constantly and significantly lower in amphiphysin $1^{-/-}$ synaptosomes than in WT ones (Fig. 1*E, left panel*). The parallel assay of the cycling of DNase I-labeled G-actin revealed, in both genotypes, an opposite pattern of cycling and lower G-actin levels in amphiphysin $1^{-/-}$ synaptosomes (Fig. 1*E, right panel*). These data strongly support an implication of amphiphysin 1 in actin assembly and dynamics in the synapse.

Amphiphysin 1 Directly Stimulates N-WASP-dependent Arp2/3 Actin Nucleation—We next explored a potential interaction of amphiphysin 1 with N-WASP using pulldown assays from neurons and testicular Sertoli cells. Amphiphysin 1 pulled down N-WASP both from extracts of rat brain synaptosomes (Fig. 2*A*) and from extracts of Ser-W3 cells, a rat Sertoli cell line, expressing Myc-tagged N-WASP (Fig. 2*B*). The interaction was mediated by amphiphysin 1 SH3 domain, as was the case for interaction with dynamin, a physiological binding partner of amphiphysin (Fig. 2, *A* and *B*) (11). A trace amount of N-WASP binding was detected by GST-Amph-ΔSH3 (Fig. 2*B*), which can be attributed to dimer formation of

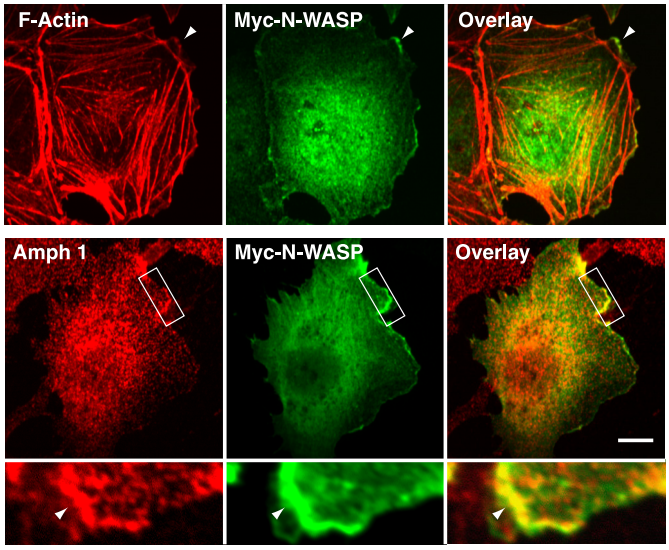

FIGURE 4. **Amphiphysin 1 and N-WASP accumulate at ruffles.** Ser-W3 cells were transfected with myc-N-WASP. After 24 h of transfection, ruffle formation was induced by stimulating PS receptors on the cell surface with 0.25 mM PS-liposomes at 37 °C for 10 min. Cells were fixed, permeabilized, and stained with anti-Myc antibodies and/or anti-amphiphysin 1 (*Amph 1*) antibodies (monoclonal antibody 3). Actin filaments were visualized by Alexa 568-phalloidin. *Arrowheads* in the *upper panel* indicate ruffles. Areas enclosed with *rectangles* in the *middle panel* were shown at higher magnification in the *lower panel*. Note that the co-localization of amphiphysin 1 and N-WASP is restricted to ruffles (*arrowheads*). *Bar,* 20 μm.

GST-Amph-ΔSH3 with endogenous amphiphysin 1. Direct interaction between N-WASP and amphiphysin 1 was demonstrated by pulldown assay using purified proteins (Fig. 2*C*).

To determine whether amphiphysin 1 directly regulates N-WASP-dependent Arp2/3 actin nucleation, formation of F-actin was quantified in an *in vitro* assay, in which pyrene-conjugated actin was incubated with N-WASP, G-actin, Arp2/3 complex, and amphiphysin. The N-WASP-triggered actin assembly was enhanced by amphiphysin 1 in a dose-dependent manner (Fig. 3*A*). In absence of N-WASP, amphiphysin 1 had no stimulatory effect on the actin assembly (Fig. 3*A*). Furthermore, *in vitro* actin polymerization assay using amphiphysin 1-deletion mutants revealed that both the N-BAR and SH3 domain of amphiphysin 1 were required for the stimulation of actin assembly. Neither the SH3 alone nor an amphiphysin 1 construct lacking the N-BAR domain (ΔN-BAR) stimulated actin assembly (Fig. 3*C*).

Amphiphysin 1/N-WASP Interaction Takes Place at Cell Periphery—To elucidate physiological significance of amphiphysin 1/N-WASP interaction, *in vivo* interaction of these molecules was examined in Ser-W3 cells. Previously, we have reported that amphiphysin 1 stimulates actin polymerization, which in turn supports ruffle formation during phagocytosis. Such ruffle formation can be induced in Sertoli cells by stimulating surface PS receptors with PS-containing liposomes (3). In PS-stimulated Ser-W3 cells, amphiphysin 1 localized at ruffles (Fig. 4) as reported previously (3). Double immunofluorescence staining of the cell revealed co-localization of amphiphysin 1 and myc-N-WASP at ruffles in particular at their very edge (Fig. 4).

Next, physiological relevance of the amphiphysin 1-N-WASP complex was examined in PS-stimulated Ser-W3 cells. Dysfunction of N-WASP by wiskostatin drastically reduced PS-dependent ruffle formation (Fig. 5*A*). Expression of mCherry-PRD of N-WASP inhibited recruitment of amphiphysin 1 to the cell periphery and reduced the ruffle formation more than 50% (Fig. 5*B*). Expression of ΔN-BAR of amphiphysin 1 also strongly inhibited the ruffle formation (Fig. 5*C*). These results suggest that amphiphysin 1 and N-WASP, at least partially, contribute to PS-dependent ruffle formation.

To investigate the temporal and spatial association of amphiphysin 1 with N-WASP in Ser-W3 cells, FRET-FLIM was performed (27, 32). First, we proved sensitivity of the method by demonstrating the homotypic interaction of amphiphysin 1 to form a homodimer. Homodimerization of amphiphysin 1 has been shown by *in vivo* and *in vitro* experiments (33). This assay allows monitoring the spatio-temporal decrease of the mean fluorescence lifetime of GFP-tagged amphiphysin 1 because of the interaction of this protein with an mCherry-tagged partner. GFP-amphiphysin 1 and amphiphysin 1-mCherry were co-expressed in Ser-W3 cells, and the fluorescence lifetime of GFP-amphiphysin 1 was acquired. The average mean lifetime of GFP-amphiphysin 1 decreased from 2.48 ± 0.01 ns in cells expressing GFP-amphiphysin 1 alone ($n = 10$) to 2.40 ± 0.03 ns in co-transfected cells ($n = 14$) (Fig. 6). This decrease in lifetime is characteristic of FRET between GFP and mCherry. Considering the fact that amphiphysin 1 acts as both donor and acceptor, the decrease of the mean lifetime of GFP could be underestimated more than the actual homotypic interaction. The high resolution map of the homotypic interaction can be displayed by using the minimal fraction of donor protein involved in FRET (mf_D) (Fig. 6) (27) (see "Experimental Procedures"). The mf_D map represents the spatial distribution of the relative variation of the effective amount of interaction. In this case, the quantification is underestimated, and the three-dimensional representation highlights the differences from the control (Fig. 6*A*, *right panel*).

Next, Ser-W3 cells expressing GFP-amphiphysin 1 and mCherry-N-WASP were imaged using the FRET-FLIM assay. In the absence of PS, only one co-expressing cell showed FRET ($n = 4$). The average mean lifetime decreased from 2.48 ± 0.01 ns in cells expressing GFP-amphiphysin alone to 2.44 ± 0.01 ns in the FRET-positive cell (S.D. calculated from the spatial distribution within the single cell). In the presence of PS, nine cells expressing GFP-amphiphysin 1 and mCherry-N-WASP showed FRET ($n = 10$), and the average mean lifetime decreased to 2.42 ± 0.02 ns (S.D. calculated from the spatial distribution within the nine cells).

A representative FRET-positive cell in the presence of PS is shown in Fig. 7*A* (*arrowhead in right bottom panel*). This demonstrates that the interaction is localized at a restricted area of the cell periphery. The specificity of this interaction is revealed by the fact that cells co-expressing GFP-amphiphysin with N-WASP-mCherry (position of the acceptor changed) did not show FRET either in the absence or in the presence of PS. In this configuration, when mCherry is placed C-terminal to the N-WASP, the acceptor is likely too far away from GFP-amphiphysin or in a wrong orientation respective to the donor to allow FRET. The fact that we did not observe a significant change in the lifetime upon PS

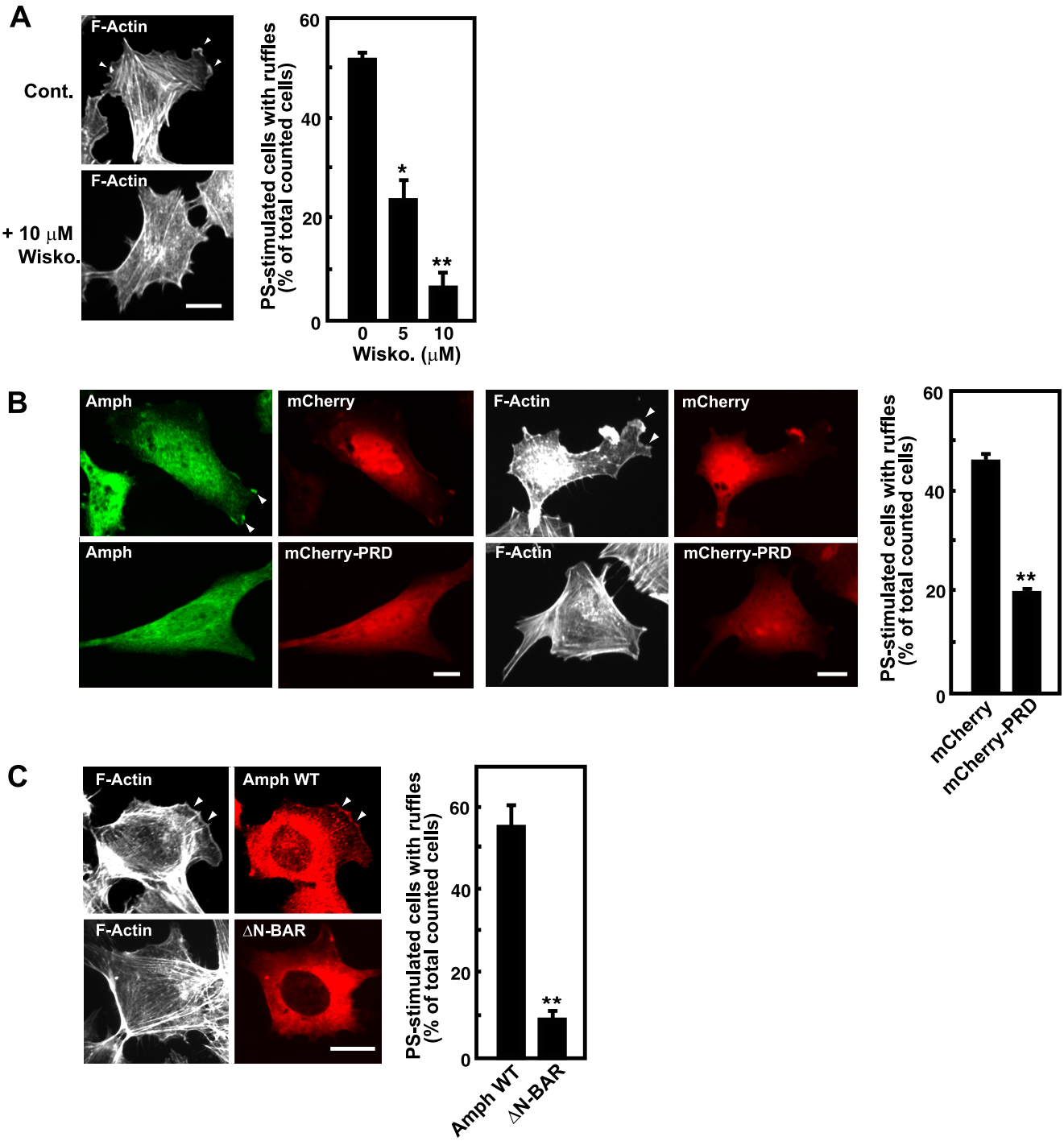

FIGURE 5. **Amphiphysin 1-N-WASP complex is involved in PS-dependent ruffle formation.** *A,* dysfunction of N-WASP causes decrease of PS-dependent ruffle formation in Ser-W3 cells. Ser-W3 cells were preincubated with or without wiskostatin (*Wisko.*) at the indicated concentrations at 37 °C for 30 min, and then cells were stimulated, and the ruffle formation was analyzed. All results represent the mean ± S.E. from the three experiments. Statistical significance was determined by Student's *t* tests (**, $p < 0.01$; *, $p < 0.05$). *Bar,* 20 μm. *B,* expression of mCherry-tagged proline-rich domain of N-WASP inhibited PS-dependent recruitment of amphiphysin 1 (*Amph*) to cell periphery in Ser-W3 cells (*B, left two columns*) and ruffle formation (*B, right two columns*). Cells were stimulated with PS-liposomes at 37 °C for 10 min. Then, endogenous amphiphysin 1 or F-actin was stained with anti-amphiphysin 1 antibodies (monoclonal antibody 3) or Alexa 488-phalloidin. *Bar,* 10 μm. *C,* effect of Myc-taggedΔN-BAR of amphiphysin 1 on PS-dependent ruffle formation was shown. Quantitative analysis for the results in *B* and *C* represents the mean ± S.E. from the three experiments. Statistical significance was determined by Student's *t* tests (**, $p < 0.01$). *Bar,* 10 μm. All the samples were examined by fluorescent confocal microscopy, and representative micrographs are shown. *Arrowheads* indicate ruffles.

addition (2.48 ± 0.01, $n = 5$) using GFP-amphiphysin/N-WASP-mCherry shows the specificity of PS addition upon the FRET signal occurring between GFP-amphiphysin and mCherry-N-WASP.

Specificity of this method was further strengthened, by confirming that the FRET signal was absent in other negative control cells as follows. In Sertoli cells co-expressing GFP-amphiphysin and mCherry, the average mean lifetime after

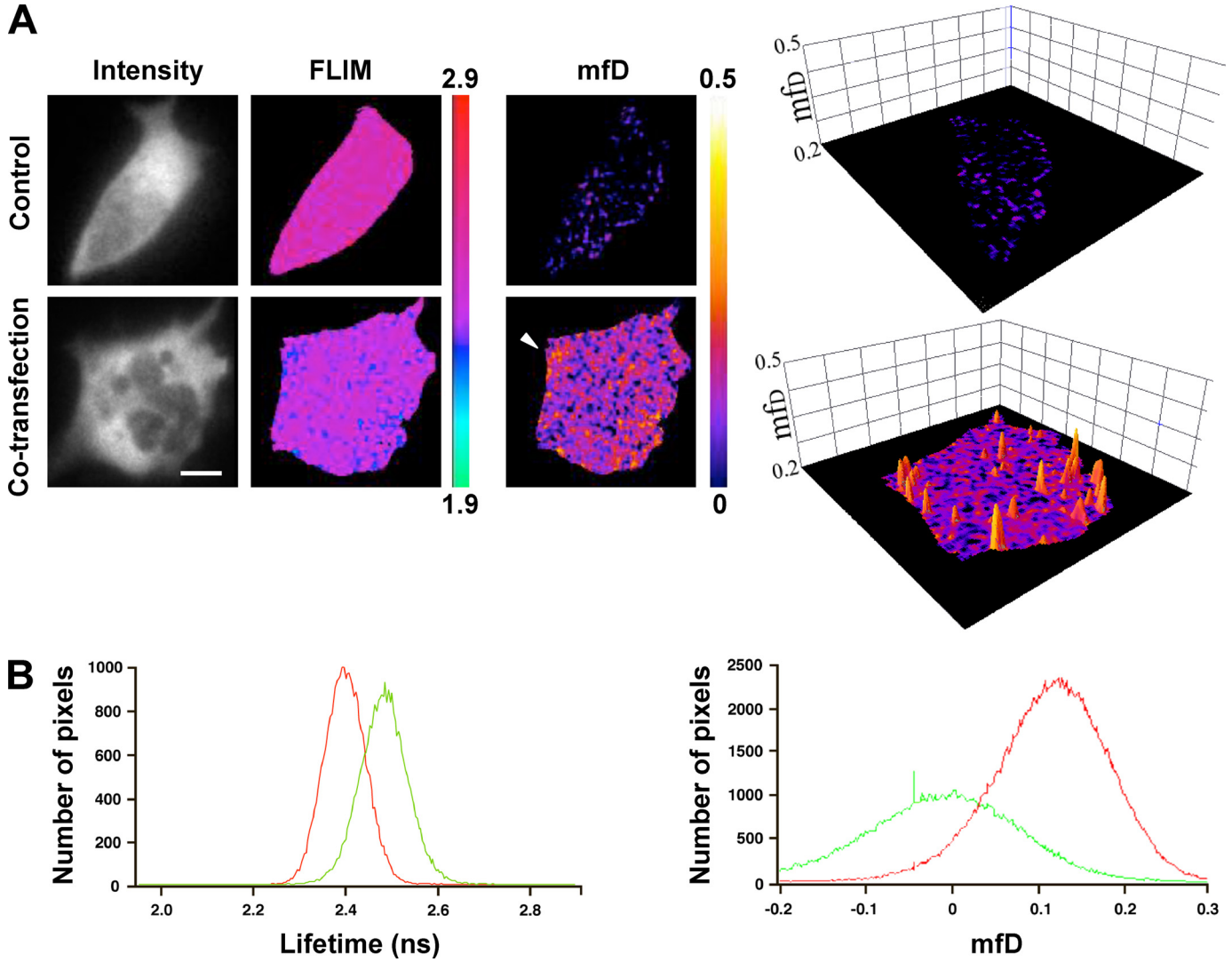

FIGURE 6. **Dimerization of amphiphysin 1 in Ser-W3 cell by FRET-FLIM.** *A*, dimerization of amphiphysin 1 in Ser-W3 cells. FLIM and minimal fraction of donor engaged in FRET (mf_D) images of GFP-amphiphysin expressed alone as control (*upper panel*) or with amphiphysin 1-mCherry (*lower panel*) were obtained using TriMscope as described under "Experimental Procedures." Three-dimensional representation of mf_D images was obtained using a threshold limit given by the control (0.2). GFP-lifetime decreased in the presence of amphiphysin 1-mCherry. *Bar*, 10 μm. *B*, lifetime (*left panel*) and mf_D histograms (*right panel*) of the control (*green*) and the co-transfection (*red*) cells show a decrease of the GFP lifetime from 2.48 ns (control) to 2.41 ns (co-expression) and the mean value of mf_D from 0 (control) to 0.11 (co-expression).

PS stimulation was 2.47 ± 0.01 ns ($n = 5$). Thus, it was very likely that the FRET signal occurring between GFP-amphiphysin and mCherry-N-WASP represents the interaction between amphiphysin and N-WASP in living cells.

Using this approach, we were able to quantify and follow the interaction in time in the presence of PS. For each cell analyzed, 20 FRET-FLIM images were sequentially acquired every 12 s, the time required for one image acquisition. From these FRET-FLIM time lapses, the spatio-temporal variations of the amount of the interaction were imaged by mf_D time lapses (for one example see supplemental Movie S1). Snapshots of the interaction are displayed in Fig. 7*C* for sequential time lag numbers 5–7 over the 20 acquisitions. These mf_D images reveal the localized and transient interaction between GFP-amphiphysin 1 and mCherry-N-WASP. Even if we measure the minimal fraction of donor engaged in FRET, because the GFP/mCherry ratio likely does not change during time lapse course (4 min), the spatio-temporal changes of mf_D within single cells represent the dynamic changes of the amount of interacting donor. The time axis profile of one representative time-lapse acquisition of a co-transfected cell in the presence of PS are shown in Fig. 7*D*.

This profile shows that the mean amount of interacting donor increases by a factor of 2 within 1 min (Fig. 7*D, 1st peak*) followed by a decrease in 12 s. After a stable period for 1 min, rapid increase to the second peak is observed (Fig. 7*D*). The rough correlation of this stimulated interaction with the time course of ruffle formation, within 10 min, suggests a role in the control of the actin nucleation that underlies their generation and dynamics. Thus, these findings provide a mechanistic explanation for our previous observation that PS-stimulated ruffling and phagocytosis was strongly impaired in Sertoli cells of amphiphysin $1^{-/-}$ mice.

DISCUSSION

Until this study, although a functional link between amphiphysin and actin had been identified, the underlying mech-

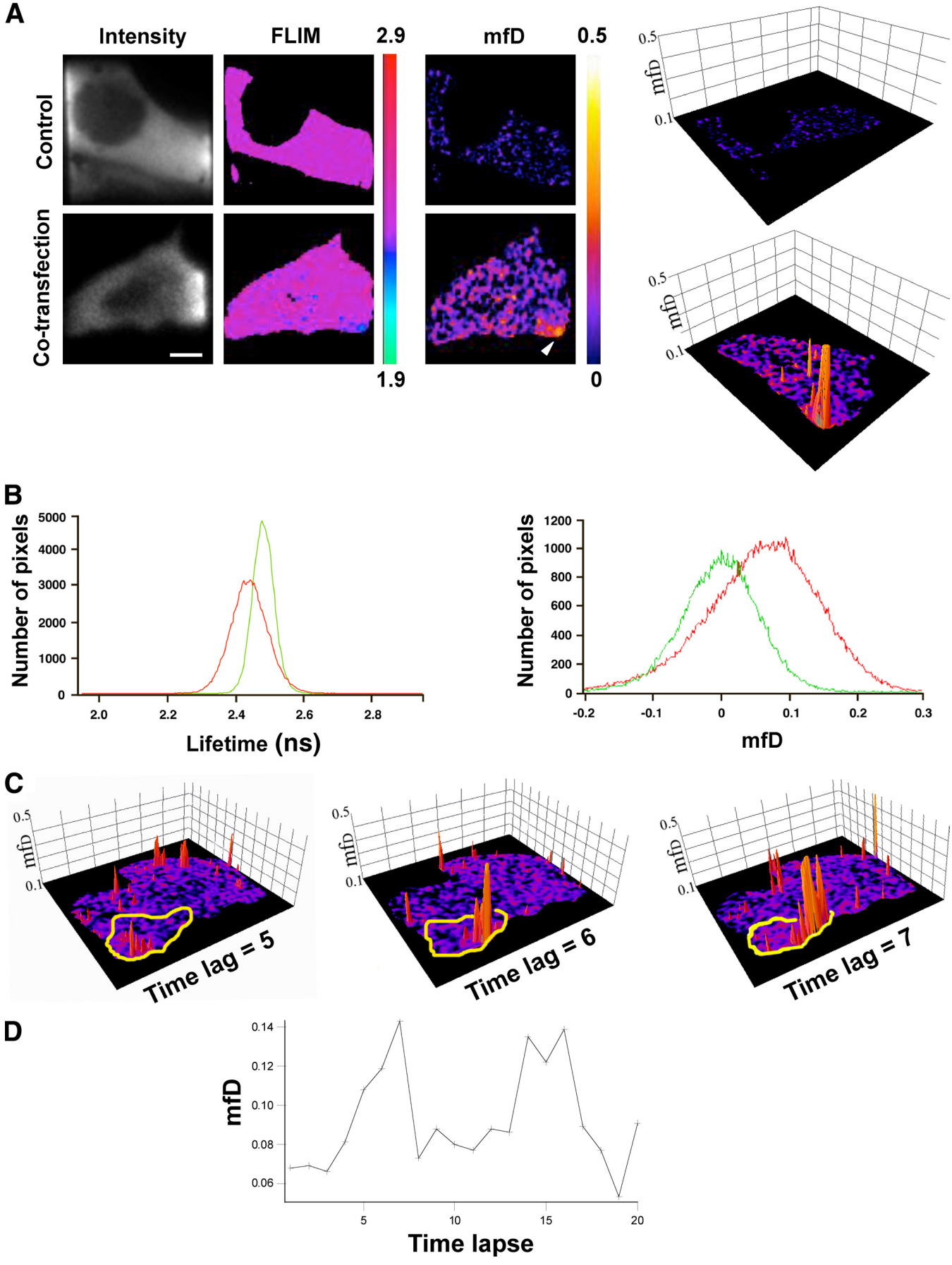
A
Intensity
FLIM
2.9
mfD
0.5
Control
Co-transfection
1.9
0
0.5
mfD
0.1
B
Number of pixels
5000
4000
3000
2000
1000
0
2.0
2.2
2.4
2.6
2.8
Lifetime (ns)
Number of pixels
1200
1000
800
600
400
200
0
-0.2
-0.1
0
0.1
0.2
0.3
mfD
C
Time lag = 5
Time lag = 6
Time lag = 7
D
mfD
0.14
0.12
0.10
0.08
0.06
5
10
15
20
Time lapse

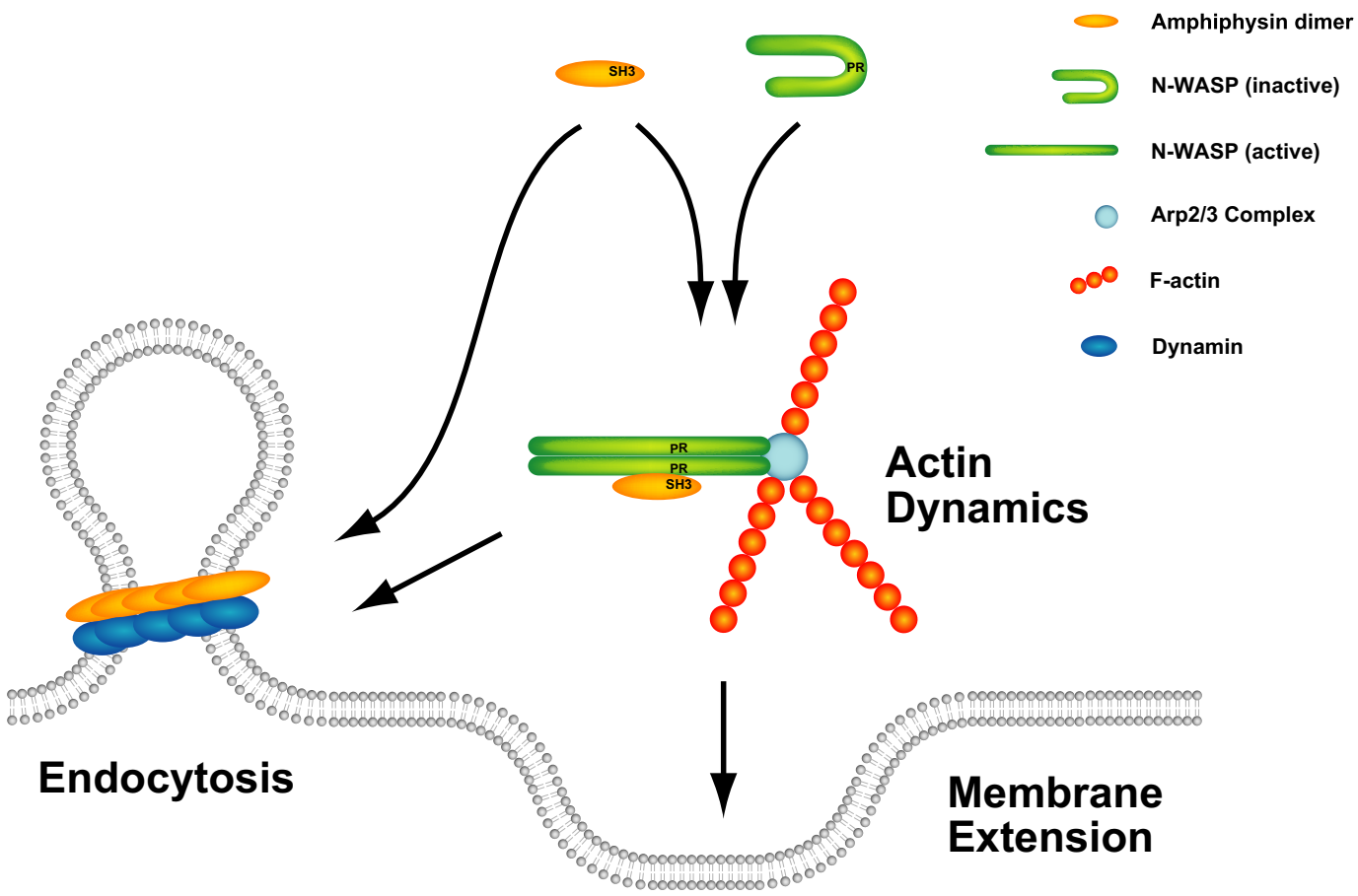

FIGURE 8. **Possible role of amphiphysin 1-N-WASP complex in actin assembly.** N-WASP is activated upon binding to the amphiphysin dimer, and the complex induces Arp2/3-dependent actin assembly. This interaction occurs in proximity to the plasma membrane where polymerized actin network may assist dynamin-dependent endocytosis or support ruffle formation. For simplification, coat components and other actin related proteins are omitted.

anistic link had remained elusive (12–15). Our results prove that amphiphysin, like other SH3 domain-containing proteins, functions as an activator of N-WASP, although additional more indirect connections to actin function are also possible. Several other SH3 domain-containing proteins that, like amphiphysin, also contain modules of the BAR domain superfamily were previously shown to stimulate actin nucleation via N-WASP and Arp2/3 *in vitro* (34–37). Furthermore, we have used FRET-FLIM to provide evidence that amphiphysin 1/N-WASP interaction occurs in a living cell and that it is enhanced at the cell periphery by a stimulus that induces ruffles formation. The multiplicity of factors that regulate the activation of N-WASP is explained by the many different contexts in which N-WASP must function.

The profound impact of amphiphysin 1 on actin nucleation in brain and Sertoli cells, as genetically shown by studies in synaptosomes (this study) or in Sertoli cells (3) of amphiphysin $1^{-/-}$ mice, likely reflects the abundance of amphiphysin 1 in these cells. Amphiphysin $1^{-/-}$ mice exhibit cognitive defects (16). It is therefore of interest to note that mutations in several genes encoding actin-regulatory proteins, including the BAR and SH3 domain-containing protein oligophrenin 1 (7, 38, 39), are responsible for inherited cases of mental retardation in humans.

Stimulation of N-WASP-dependent actin assembly required, surprisingly, not only the SH3 domain but also the N-BAR domain (Fig. 3*C*). The BAR domain is responsible both for homo- or heterodimerization of amphiphysin (33) and for lipid bilayer binding (7, 8). The property of amphiphysin 1 stimulates N-WASP-dependent actin assembly even in the absence of liposomes (Fig. 3, *A* and *C*). These results strongly suggest that dimerization but not membrane

FIGURE 7. **Spatio-temporal association of amphiphysin 1 with N-WASP.** *A,* amphiphysin 1/N-WASP interaction. FLIM and mf_D images of GFP-amphiphysin 1 expressed alone as control (*upper panel*) or with mCherry-N-WASP (*lower panel*) present a localized decrease at the periphery of the cell (shown by *arrowhead*). Three-dimensional mf_D image (threshold limit of 0.1 given by the control) highlights the localization and its extent (up to 0.30 for this example). *Bar,* 10 μm. *B,* lifetime (*left panel*) and mf_D histograms (*right panel*) of control (*green*) and co-transfected (*red*) cells show a lifetime and mf_D variation from 2.48 ns (control) to 2.43 ns (co-expression) and from 0 (control) to 0.09 (co-expression), respectively. *C,* time-lapse of amphiphysin 1/N-WASP interaction. GFP-amphiphysin 1 expressed with mCherry-N-WASP in Ser-W3 cell was imaged and captured every 12 s during 240 s using the TriM-FLIM system. Time-lapse of the 20 mf_D images is presented in supplemental Movie S1. Here, three-dimensional images of mf_D values at time 60, 72, and 84 s are shown (threshold limit of 0.1 given by the control), exhibiting the increase of transient localized amphiphysin 1/N-WASP interaction at the periphery of the cell. *D,* time profile of the region of interest shown in *C* during all the time-lapse experiments presents two consecutive peaks for amphiphysin 1/N-WASP transient interaction (time lag 7 (84 s) and time lag 15 (180 s)) at the same region of the cell.

binding may be crucial for the activation. One potential explanation of this finding is that dimerization may in turn promote the clustering and dimerization of N-WASP. A recent study has shown that full activation of N-WASP requires its dimerization following its allosteric relief of autoinhibition by regulatory factors such as SH3 domains and that dimeric SH3 domains are much more powerful activators than monomeric SH3 domains (40). In any case, because full N-WASP activation requires its binding to $PI(4,5)P_2$ in the plasma membrane, the physiological sites of these interactions is the cell cortex. Several previous studies of amphiphysin 1 have focused on its role in endocytosis. The current model is that the curvature-generating and curvature-sensing properties of the N-BAR domain of amphiphysin mediate its accumulation at the neck of endocytic pits. In endocytosis, amphiphysin 1 couples clathrin-mediated budding to fission and clathrin uncoating. In the former process, amphiphysin 1 binds to clathrin and AP-2, the clathrin adaptor, and in the latter process it binds to dynamin and to the $PI(4,5)P_2$ phosphatase synaptojanin via its SH3 domain (6, 11). However, it is now clear that actin and endocytosis, including clathrin-mediated endocytosis, are intimately interconnected and that actin also assembles at the neck of at least a subset of clathrin-coated pits (Fig. 8) (15, 41). Thus, amphiphysin may function in cooperation with other BAR superfamily proteins that also contain SH3 domains to induce curvature-dependent actin polymerization at the neck of endocytic pits (34–37). Evidence for a role of amphiphysin in ruffles and the occurrence of isoforms of amphiphysin that lack the clathrin and AP-2-binding motifs indicate that endocytosis-independent actions may occur (42, 43). Our identification of a role for the BAR domain of amphiphysin independent from bilayer binding further supports this possibility. In conclusion, we have shown here that amphiphysin 1 is an important regulator of actin polymerization through its interaction with N-WASP and that this interaction is regulated in time and space.

Acknowledgments—We thank Dr. Tsien (Howard Hughes Medical Institute, University of California, San Diego) for mCherry constructs, Dr. Scita (Istituto Fondazione Italiana Ricerca sul Cancro di Oncologia Molecolare Via Adamello 16, Italy) for anti-PAN-WAVE antibodies, and Dr. Kirschner (Harvard Medical School, Boston) for anti-N-WASP antibodies. We also thank the Imaging Facilities of the Institut Jacques Monod.

REFERENCES

1. Pollard, T. D., and Borisy, G. G. (2003) *Cell* **112,** 453–465
2. Takenawa, T., and Suetsugu, S. (2007) *Nat. Rev. Mol. Cell Biol.* **8,** 37–48
3. Yamada, H., Ohashi, E., Abe, T., Kusumi, N., Li, S. A., Yoshida, Y., Watanabe, M., Tomizawa, K., Kashiwakura, Y., Kumon, H., Matsui, H., and Takei, K. (2007) *Mol. Biol. Cell* **18,** 4669–4680
4. De Camilli, P., Thomas, A., Cofiell, R., Folli, F., Lichte, B., Piccolo, G., Meinck, H. M., Austoni, M., Fassetta, G., Bottazzo, G., Bates, D., Cartlidge, N., Solimena, M., and Kilimann, M. W. (1993) *J. Exp. Med.* **178,** 2219–2223
5. Watanabe, M., Tsutsui, K., Hosoya, O., Tsutsui, K., Kumon, H., and Tokunaga, A. (2001) *Biochem. Biophys. Res. Commun.* **287,** 739–745
6. Cestra, G., Castagnoli, L., Dente, L., Minenkova, O., Petrelli, A., Migone, N., Hoffmüller, U., Schneider-Mergener, J., and Cesareni, G. (1999) *J. Biol. Chem.* **274,** 32001–32007
7. Peter, B. J., Kent, H. M., Mills, I. G., Vallis, Y., Butler, P. J., Evans, P. R., and McMahon, H. T. (2004) *Science* **303,** 495–499
8. Yoshida, Y., Kinuta, M., Abe, T., Liang, S., Araki, K., Cremona, O., Di Paolo, G., Moriyama, Y., Yasuda, T., De Camilli, P., and Takei, K. (2004) *EMBO J.* **23,** 3483–3491
9. Slepnev, V. I., Ochoa, G. C., Butler, M. H., and De Camilli, P. (2000) *J. Biol. Chem.* **275,** 17583–17589
10. Schmid, S. L., McNiven, M. A., and De Camilli, P. (1998) *Curr. Opin. Cell Biol.* **10,** 504–512
11. Takei, K., Slepnev, V. I., Haucke, V., and De Camilli, P. (1999) *Nat. Cell Biol.* **1,** 33–39
12. Mundigl, O., Ochoa, G. C., David, C., Slepnev, V. I., Kabanov, A., and De Camilli, P. (1998) *J. Neurosci.* **18,** 93–103
13. Sivadon, P., Bauer, F., Aigle, M., and Crouzet, M. (1995) *Mol. Gen. Genet.* **246,** 485–495
14. Munn, A. L., Stevenson, B. J., Geli, M. I., and Riezman, H. (1995) *Mol. Biol. Cell* **6,** 1721–1742
15. Kaksonen, M., Toret, C. P., and Drubin, D. G. (2005) *Cell* **123,** 305–320
16. Di Paolo, G., Sankaranarayanan, S., Wenk, M. R., Daniell, L., Perucco, E., Caldarone, B. J., Flavell, R., Picciotto, M. R., Ryan, T. A., Cremona, O., and De Camilli, P. (2002) *Neuron* **33,** 789–804
17. Miki, H., Miura, K., and Takenawa, T. (1996) *EMBO J.* **15,** 5326–5335
18. Suetsugu, S., Miki, H., and Takenawa, T. (1998) *EMBO J.* **17,** 6516–6526
19. Egile, C., Loisel, T. P., Laurent, V., Li, R., Pantaloni, D., Sansonetti, P. J., and Carlier, M. F. (1999) *J. Cell Biol.* **146,** 1319–1332
20. Park, S. J., Suetsugu, S., and Takenawa, T. (2005) *EMBO J.* **24,** 1557–1570
21. Kinuta, M., Yamada, H., Abe, T., Watanabe, M., Li, S. A., Kamitani, A., Yasuda, T., Matsukawa, T., Kumon, H., and Takei, K. (2002) *Proc. Natl. Acad. Sci. U.S.A.* **99,** 2842–2847
22. Kamitani, A., Yamada, H., Kinuta, M., Watanabe, M., Li, S. A., Matsukawa, T., McNiven, M., Kumon, H., and Takei, K. (2002) *Biochem. Biophys. Res. Commun.* **294,** 261–267
23. Lebensohn, A. M., Ma, L., Ho, H. Y., and Kirschner, M. W. (2006) *Methods Enzymol.* **406,** 156–173
24. Dunkley, P. R., Heath, J. W., Harrison, S. M., Jarvie, P. E., Glenfield, P. J., and Rostas, J. A. (1988) *Brain Res.* **441,** 59–71
25. Bernstein, B. W., and Bamburg, J. R. (1989) *Neuron* **3,** 257–265
26. Ma, L., Cantley, L. C., Janmey, P. A., and Kirschner, M. W. (1998) *J. Cell Biol.* **140,** 1125–1136
27. Padilla-Parra, S., Audugé, N., Coppey-Moisan, M., and Tramier, M. (2008) *Biophys. J.* **95,** 2976–2988
28. Ho, H. Y., Rohatgi, R., Lebensohn, A. M., Le Ma, Li, J., Gygi, S. P., and Kirschner, M. W. (2004) *Cell* **118,** 203–216
29. Peterson, J. R., Bickford, L. C., Morgan, D., Kim, A. S., Ouerfelli, O., Kirschner, M. W., and Rosen, M. K. (2004) *Nat. Struct. Mol. Biol.* **11,** 747–755
30. Bauerfeind, R., Takei, K., and De Camilli, P. (1997) *J. Biol. Chem.* **272,** 30984–30992
31. Wegner, A. M., Nebhan, C. A., Hu, L., Majumdar, D., Meier, K. M., Weaver, A. M., and Webb, D. J. (2008) *J. Biol. Chem.* **283,** 15912–15920
32. Tramier, M., Gautier, I., Piolot, T., Ravalet, S., Kemnitz, K., Coppey, J., Durieux, C., Mignotte, V., and Coppey-Moisan, M. (2002) *Biophys. J.* **83,** 3570–3577
33. Wigge, P., Köhler, K., Vallis, Y., Doyle, C. A., Owen, D., Hunt, S. P., and McMahon, H. T. (1997) *Mol. Biol. Cell* **8,** 2003–2015
34. Otsuki, M., Itoh, T., and Takenawa, T. (2003) *J. Biol. Chem.* **278,** 6461–6469
35. Kessels, M. M., and Qualmann, B. (2004) *J. Cell Sci.* **117,** 3077–3086
36. Yarar, D., Waterman-Storer, C. M., and Schmid, S. L. (2007) *Dev. Cell* **13,** 43–56
37. Takano, K., Takano, K., Toyooka, K., and Suetsugu, S. (2008) *EMBO J.* **27,** 2817–2828
38. Billuart, P., Bienvenu, T., Ronce, N., des Portes, V., Vinet, M. C., Zemni, R., Roest Crollius, H., Carrié, A., Fauchereau, F., Cherry, M., Briault, S., Hamel, B., Fryns, J. P., Beldjord, C., Kahn, A., Moraine, C., and Chelly, J. (1998) *Nature* **392,** 923–926
39. Itoh, T., and De Camilli, P. (2006) *Biochim. Biophys. Acta* **1761,**

897–912
40. Padrick, S. B., Cheng, H. C., Ismail, A. M., Panchal, S. C., Doolittle, L. K., Kim, S., Skehan, B. M., Umetani, J., Brautigam, C. A., Leong, J. M., and Rosen, M. K. (2008) *Mol. Cell* **32,** 426–438
41. Merrifield, C. J., Perrais, D., and Zenisek, D. (2005) *Cell* **121,** 593–606
42. Gold, E. S., Morrissette, N. S., Underhill, D. M., Guo, J., Bassetti, M., and Aderem, A. (2000) *Immunity* **12,** 285–292
43. Lee, E., Marcucci, M., Daniell, L., Pypaert, M., Weisz, O. A., Ochoa, G. C., Farsad, K., Wenk, M. R., and De Camilli, P. (2002) *Science* **297,** 1193–1196
44. Rohatgi, R., Ma, L., Miki, H., Lopez, M., Kirchhausen, T., Takenawa, T., and Kirschner, M. W. (1999) *Cell* **97,** 221–231